PHYSICAL REVIEW B **83**, 195414 (2011)

Normal-incidence x-ray standing-wave study of copper phthalocyanine submonolayers on Cu(111) and Au(111)

Ingo Kröger,[1] Benjamin Stadtmüller,[1] Christoph Kleimann,[1] Parasmani Rajput,[2] and Christian Kumpf[1]
[1]*Peter Grünberg Institut (PGI-3), Forschungszentrum Jülich, D-52425 Jülich, Germany, and JARA Fundamentals of Future Information Technology (JARA-FIT), D-52425 Jülich, Germany*
[2]*European Synchrotron Radiation Facility, 6 rue Jules Horowitz, F-38043 Grenoble Cedex 9, France*
(Received 15 February 2011; published 6 May 2011)

Understanding the adsorption and growth mechanisms of large π-conjugated molecules on noble metal surfaces is a crucial aspect for designing and optimizing electronic devices based on organic materials. The investigation of adsorption heights for these molecules on different surfaces can be a direct measure for the strength of the adsorbate-substrate interaction, and gives insight into the fundamental bonding mechanisms. However, the adsorption strength is often also influenced by intermolecular (lateral) interactions which cause, e.g., island formation in the submonolayer regime and influence the adsorption geometry of individual molecules. The lateral structure can then dominate the vertical structure formation and influence the adsorbate-substrate interaction. In this context, the adsorption of copper-phthalocyanines on noble metal surfaces [Au(111), Ag(111), and Cu(111)] represents an ideal model system since the lateral structure formation, as well as the molecular adsorption geometries, strongly depend on coverage and temperature, and hence can be tuned easily. We demonstrate that for CuPc/Au(111), a system dominated by physisorption, the adsorption height of the molecules is independent from the lateral adsorption geometry. In contrast, a strong chemisorption of CuPc on Cu(111) shows a clear gradient in the interaction strength: Individual molecules in diluted phases are significantly stronger bonded than molecules in dense phases. This finding quantifies the increase of the exchange correlation in the binding process, which goes along with the tendency to a more site-specific adsorption geometry at small coverages.

DOI: 10.1103/PhysRevB.83.195414 PACS number(s): 68.43.Fg, 68.49.Uv

I. INTRODUCTION

During past years, the growth of large π-conjugated molecules on noble metal surfaces has attracted much interest in the surface science community (see, e.g., Refs. 1–4 and references therein). In particular, model systems like perylene and related molecules [the most popular one is perylene-3,4,9,10-tetracarboxylic-dianhydride (PTCDA)],[5–14] but also the (metal-) phthalocyanines (MePc) and similar molecules were in the focus of many experimental and theoretical studies.[15–21]

One important goal of such studies was the investigation of the metal-organic interface. Its geometric properties are crucial for further growth of multilayer films, for the film morphology, but also for electronic properties like valence level alignment, band bending, etc.[22] In this context, type and strength of the adsorbate-substrate interaction plays a decisive role. It is directly correlated with the charge transfer at the interface and the epitaxial growth in the submonolayer regime.

While spectroscopic methods often allow one to directly measure the charge transfer between molecules and substrate, there are not many techniques which allow one to determine the *vertical* geometric structure of the adsorbate system with such precision that conclusions on the interaction strength can be drawn. One such technique is (normal-incidence) x-ray standing waves (NIXSW),[23–27] which enables access to adsorption heights of individual atoms (or at least groups of atoms of the same type) within a molecule. This allows one to analyze the bonding between molecule and substrate, identify those functional groups mediating the bonding, or detect a bending of the molecules. These data also often represent a benchmark for state of the art quantum chemical calculations. Also, in this context, the adsorption of PTCDA on the noble metal surfaces Ag(111), Au(111), and Cu(111) represents a model system and was well investigated in the past. Fundamental insights into the adsorbate-substrate interactions[4,7,8,28–30] were achieved for all known phases in the monolayer-coverage range including a metastable low-temperature (LT) phase of PTCDA on Ag(111).[9] For the latter, it was shown that the molecular alignment with the substrate (and hence the adsorption geometry) has strong impact on the bonding strength. However, since only very few discrete phases occur, the correlation of lateral structure and (vertical) interaction strength can only be studied punctually. For a more comprehensive and consistent investigation, an adsorbate system is needed which allows one to "tune" the lateral adsorption geometry and thus study the consequences for the vertical structure in a wider range.

The adsorption of MePc molecules on noble metal surfaces represents such a system, since it shows a wide variety of phases in the submonolayer regime, the formation of which can be precisely controlled by coverage and temperature. In several studies, we have investigated mostly SnPc and CuPc and their adsorption on Ag(111).[19,31,32] Within this paper, we continue our work on CuPc/Au(111) and CuPc/Cu(111).[33]

The occurrence of intermolecular repulsion in a certain coverage regime of approximately 0.9–1.0 monolayers (ML) is a common feature of SnPc and CuPc (and possibly also other phthalocyanine molecules) adsorbed on Ag(111).[19,31,32] This effect manifests itself in a series of long-range-ordered structures, which change their unit cell parameters continuously with increasing coverage. For CuPc/Ag(111), these structures have point-on-line (p.o.l.) coincidence with the substrate and show a weaker bonding for higher coverages compared to more isolated molecules at low coverages. At a coverage of 0.5 ML,

where the molecules form a disordered phase and occupy their favorable adsorption site in a well-aligned geometry with high symmetry directions of the substrate, their adsorption height is approximately 3%–4% smaller than in the monolayer structure with a closely compressed (lateral) packing of molecules with many different adsorption sites.[32] This clearly indicates the impact of the lateral structure of the overlayer on the vertical bonding which—in close-packed configurations—hinders the spatial overlap of molecular wave functions with the substrate in this case of weak chemisorption.

In a subsequent study, we investigated the lateral adsorbate structure as well as the electronic valence structure of submonolayer phases of CuPc on Au(111) and Cu(111).[33] On Au(111), the CuPc molecules adsorb in a gaseous phase in a wide range of coverages up to 0.93 ML. Above this value they form several very similar p.o.l. structures with almost identical unit cell sizes. A phase transition to a LT phase was also found, but while this phase is commensurate for CuPc/Ag(111), in the case of Au(111), it shows only p.o.l. coincidence. This indicates that there is no strong tendency for site-specific adsorption. Photoelectron spectroscopy measurements also approve a weaker adsorbate-substrate interaction for the CuPc adsorption on Au(111) than on Ag(111).[33]

The adsorption behavior of CuPc on Cu(111) is principally different from that on Ag(111) and Au(111). On Cu(111), the molecules show short-range intermolecular attraction at all coverages.[33] Below 0.76 ML, this is indicated by the formation of chains that were observed in LT scanning tunneling microscopy (STM).[18] At higher coverage, CuPc shows "conventional" island growth in a centered orthorhombic superstructure with two molecules per unit cell. The intermolecular attraction was explained by a breaking of the fourfold symmetry of the molecule due to charge transfer, which induces a quadrupole moment in the molecules. This quadrupole moment overcompensates any intermolecular repulsion that could be expected from the results on the Ag surface. Supporting results were found by Wang *et al.*[20] in LT-STM investigations of SnPc/Ag(111). Here one has to distinguish Sn-up and Sn-down configurations since the molecule is not planar. Sn-up molecules have a smaller overlap of molecular wave functions with the substrate and hence show a weaker donation/back-donation effect than Sn-down oriented molecules. This makes repulsive interaction—as it was described in Refs. 19, 31, and 32—dominant for Sn-up molecules. But in Sn-down orientation the induced quadrupole moment already prevails and leads to intermolecular attraction, indicated by the formation of molecular chains similar to CuPc/Cu(111).[18] These investigations demonstrate the interrelation of intermolecular interaction (attraction or repulsion), strength of the bonding of the molecules to the substrate (physisorption or chemisorption), and the effects which are responsible for the lateral structure formation (adsorption sites, steric conditions, etc.).

In this context, the NIXSW investigations on selected submonolayer phases of CuPc on Au(111) and Cu(111), which are the subject of the present paper, represent an essential (and possibly final) piece of information which allows one to qualify and quantify the adsorbate-substrate interaction and complete the fundamental understanding of this interesting adsorbate system.

II. EXPERIMENT

NIXSW experiments were performed at the ID32 beamline of the European Synchrotron Radiation Facility (ESRF) in Grenoble, France, using unfocused radiation and a Si(111) monochromator ($\Delta E/E = 1.3 \times 10^{-4}$) in back reflection geometry.[34] The local ultrahigh vacuum chamber was equipped with a hemispherical electron analyzer (Perkin-Elmer PHI model 10-360, $r = 150$ mm) at an angle of 45° to the incident beam, and all equipment necessary for sample preparation. The base pressure during the experiments was below 5×10^{-10} mbar. The substrate crystal surfaces were prepared by repeated Ar-ion sputtering and subsequent annealing at 923 K for 30 or 45 min. The cleanness of the surfaces was confirmed by x-ray photoelectron spectroscopy (XPS) and, in case of the Au(111), also by low energy electron diffraction (LEED) using the $22 \times \sqrt{3}$ reconstruction. CuPc films were grown by molecular-beam epitaxy and monitoring with a quadrupole mass spectrometer. Subsequently, the films on Au(111) were annealed at 553 K and those on Cu(111) at 433 K for 20 min. The coverages were determined from the integrated C1*s* XPS signal as well as from the LEED images which are well known for all submonolayer phases.[33] The corresponding phase diagram reported there was well reproduced.

In the following we briefly introduce the fundamentals of the NIXSW method. A more detailed description can be found in literature.[23–27]

A standing wave field is generated by the superposition of an incident and Bragg reflected x-ray wave from a crystal surface, when the Bragg condition for a $\vec{H} = (hkl)$ reflection is fulfilled. While scanning the photon energy through the Bragg condition ("XSW-scan"), the relative phase between the incident and reflected beam shifts by π, leading to a spatial shift of the standing wave field by half a lattice parameter d_{hkl}. Hence the spatial positions of nodes and antinodes (in the direction perpedicular to the Bragg plane) depend strongly on the photon energy. Antinodes are shifted from a position on the lattice planes to a position in between during an XSW scan. Consequently, the photoelectron yield of any atomic species in the standing wave changes accordingly and reflects the position of the atomic species relative to the lattice planes. The photoelectron yield $I(E)$ can be written as[24–27]

$$I(E) = 1 + S_R R + 2|S_I|\sqrt{R} \cdot F^H \cos(\nu - 2\pi P^H + \Psi), \quad (1)$$

with

$$S_R = \frac{1+Q}{1-Q}, \quad |S_I| = \frac{\sqrt{1+Q^2\tan^2\Delta}}{1-Q}, \quad (2)$$

and

$$\Psi = \tan^{-1}(Q\tan\Delta). \quad (3)$$

The coherent position P^H and coherent fraction F^H are the fitting parameters in this formula. P^H represents the average position of the atomic species in question and is given in units of the lattice spacing d_h: $P^H = \frac{D^H}{d_h}$. The coherent fraction F^H measures the width of the distribution of their positions. $F^H = 1$ corresponds to only one atomic position (or several equivalent ones), while $F^H = 0$ reflects a random distribution of atomic heights. The reflected beam intensity $R(E)$, its

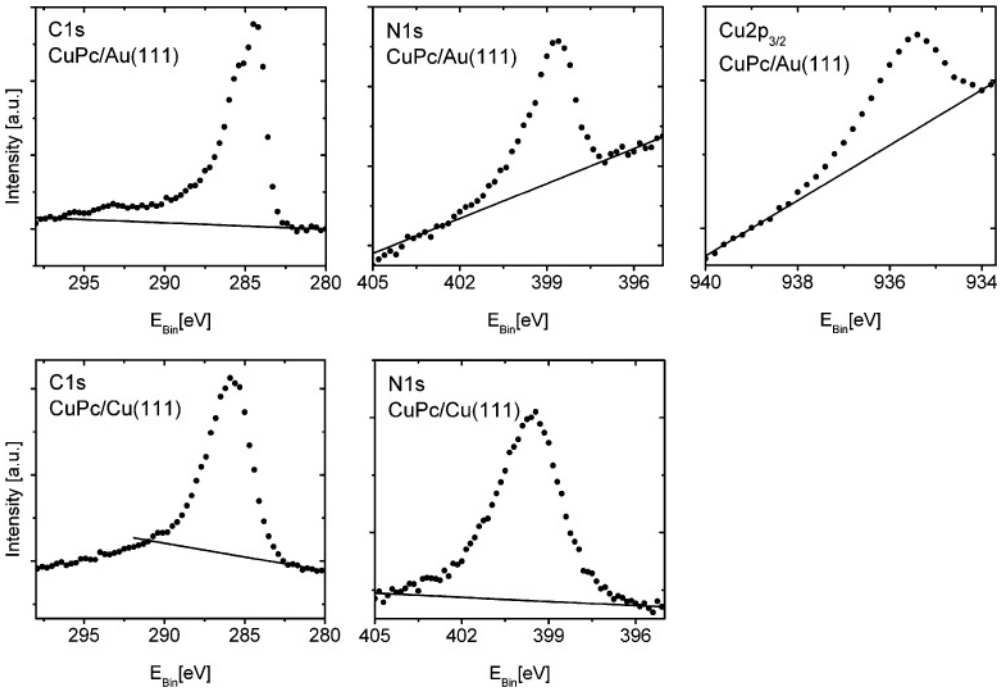

FIG. 1. Exemplary XPS spectra of the investigated species.

complex amplitude $\sqrt{R(E)}$, and relative phase $\nu(E)$ can be derived from fitting the measured reflectivity curve, whereby a Gaussian energy broadening (instrumentation function) must be taken into account. For fitting the reflectivity, the atomic form factors for forward (000) and backward scattering (111 reflection) are needed: $f = f_0 + f' + if''$. From Refs. 35 and 36, we derived $f_{0,\mathrm{forw}} = 79$, $f_{0,\mathrm{backw}} = 66.25$, $f' = -23.49$, and $f'' = 29.20$ for Au(111) and $f_{0,\mathrm{forw}} = 29$, $f_{0,\mathrm{backw}} = 22.06$, $f' = -0.09$, and $f'' = 3.35$ for Cu(111).

The multipole parameters[24,26,27] Q and Δ are used to consider multipole effects of the photoemission process, since the dipole approximation is not valid any more for photon energies in the keV energy regime that is necessary in order to fulfill the Bragg condition. Q was derived from XSW measurements on incoherent multilayer films for which the coherent fraction F^H is 0. This reduces Eq. (1) to $I(E) = 1 + \frac{1+Q}{1-Q}R$ and enables the fitting of Q. The parameter Δ was taken from literature (see Table I). An estimation of a possible systematic error due to a false Δ value was determined to be $\leqslant 0.02$ Å, which is much smaller than the statistical error of the measurement. Note that nondipolar parameters can in principle be obtained from a comparison of photoemission-based and Auger-based XSW results.[12] However, this method was not applied within this work since correction parameters are known with sufficient precision for the species involved, and also due to limited beamtime capacities.

TABLE I. Multipole correction parameters.

		C1s	N1s	Cu2$p_{3/2}$
Ag(111): 2640 eV	Q	0.24	0.22	0.17
		Ref. 31	Ref. 31	Ref. 32
	Δ	−0.21	−0.26	−0.21
		Ref. 31	Ref. 31	Ref. 31
Cu(111): 2979 eV	Q	0.24	0.24	
	Δ	−0.21	−0.26	

The photoelectron yield curves were derived from the integrated C1s, N1s, and Cu2$p_{3/2}$ signals, considering the subtraction of a linear background (see Fig. 1). Note that a special background treatment for the C1s signal from CuPc/Cu(111) was chosen because of a noise signal stemming from the analyzer electronics in the range between 296 and 292 eV. This artifact was reproducible in all measurements and bypassed by a short integration range for the C1s signal.

Beam damage in terms of a lowering of the coherent fraction[29] was observed for thin films on Au(111) already after 10 min of synchrotron beam exposure, and after 30 min on Cu(111). Therefore, we were running many short XSW scans (5 min) on different spots of the Au(111) surface, and 20 min scans on Cu(111). This lead to limited statistics of individual measurements, in particular for the Cu2p data from the Au(111) surface. In accordance with previous error treatments[28,32] and a careful statistical treatment of these individual scans, we estimate an upper limit of the error of $\Delta D^H = 0.07$ Å and $\Delta F^H = 0.1$. However, the results shown in the following are based on the analysis of the summed spectra for many spots and therefore have much better statistics and enable very accurate fitting. They hence represent the expectation value for individual measurements on single spots.

III. RESULTS

A. CuPc on Au(111)

For CuPc on Au(111) we performed NIXSW measurements at two different coverages, 0.7 and 1.0 ML, both at room temperature (RT, 300 K) and LT (133 K in this case). According to the phase diagram (see Fig. 1 of Stadtmüller

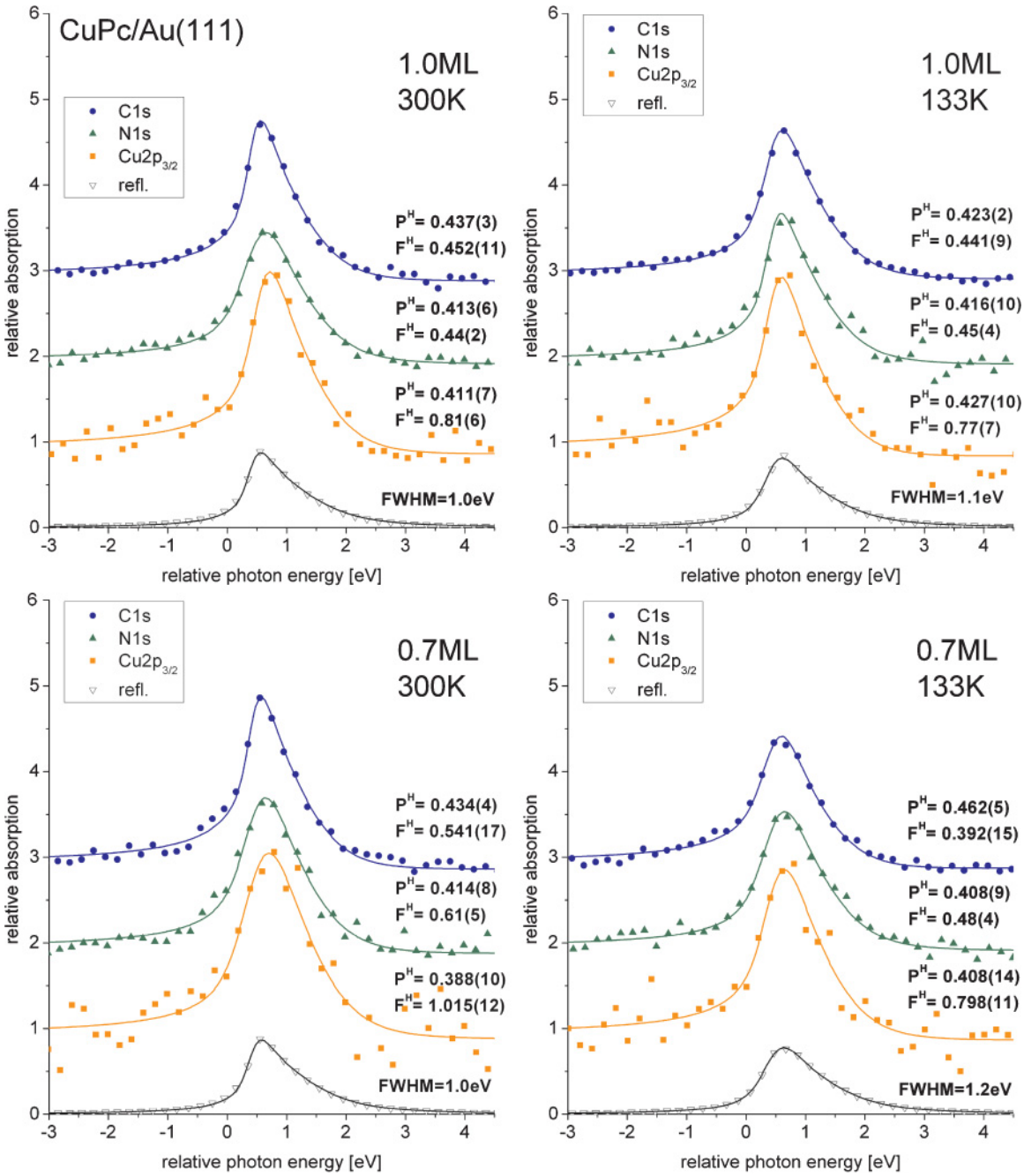

FIG. 2. (Color online) Photoelectron yield and reflectivity curves for CuPc/Au(111) (summed individual scans). The errors given here stem from the χ^2 fitting from the GMinuit algorithm in Root. More realistic values are given in Fig. 3; see also the end of Sec. II and Ref. 32.

et al.[33]), this corresponds to the so-called "*g*-phase" and "LT-phase" structures (0.7 ML, RT and LT, respectively) and the "compressed monolayer structure" (1.0 ML). For all four data sets, the C1*s*, N1*s*, and Cu2*p* photoelectron yield and corresponding reflectivity curves are shown in Fig. 2. The reflectivity shows a rather strong asymmetry, which originates from the high absorption (i.e., the large imaginary part of the atomic form factor) of the Au atoms. All photoelectron yield curves have rather similar shapes, which is also reflected by rather similar fitting results for the coherent positions P^H. This indicates that no big differences in the adsorption height of the molecules occur for different temperatures and coverages, which is a clear difference to the adsorption of CuPc on Ag(111). For that system a significantly stronger interaction between CuPc and the Ag(111) surface was found for small coverages (i.e., for molecules in diluted phases).[32] This became most obvious when the coverages 0.7 and 1.0 ML were compared. But even though the phase diagrams for CuPc on Ag(111) and Au(111) are very similar, this effect was not observed for CuPc/Au(111).

Coherent fractions are in the range 0.4–0.6 for C1*s* and N1*s*, and between 0.8 and 1.0 for Cu2*p*. They show no significant trend or variation with changing coverage and temperature. The rather high values for F^H(Cu2*p*) might partly be due to

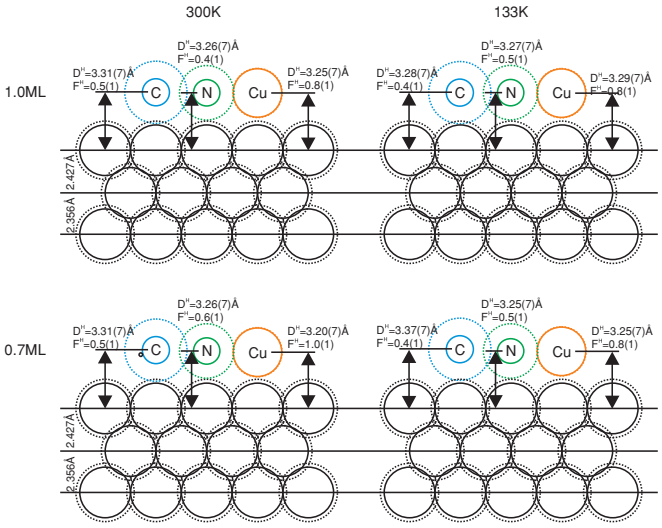

FIG. 3. (Color online) On-scale adsorption model for CuPc/Au(111). The topmost Au layer is outward relaxed by 3% of the lattice spacing. The dotted and full circles denote van der Waals[37] and covalent bonding radii,[38] respectively.

not very precise values for the Q parameter for this species, and the fact that nondipolar effects in XSW can only be corrected precisely for photoelectron emission from (spherical) s shells.

The standing-waves method measures distances (coherent positions P^H) relative to bulk lattice planes. Therefore, a relaxation of the uppermost lattice plane, 3% of the lattice spacing in the case of the Au(111) reconstruction,[39] has to be taken into account when precise bonding distances shall be determined.[29] Figure 3 shows the adsorption heights of the different molecular species in a true-scale model. The dotted circles denote noncontact (van der Waals) radii taken from Ref. 37; the full circles represent covalent bonding radii from Ref. 38. It can be seen that the bonding distances match the sum of the van der Waals radii quite accurately, in particular for the nitrogen atoms. This indicates pure physisorption on the Au substrate. Furthermore, the adsorption heights of different species are in the same range (within the error bar they are identical), which indicates that the molecules are not distorted or bent upon adsorption. A very similar adsorption height (3.27 Å) was observed for the carbon backbone of physisorbed PTCDA on Au(111).[29]

B. CuPc on Cu(111)

For the system CuPc/Cu(111), three different phases have been found in the phase diagram.[33] First, at 0.9 ML and above, the molecules form large commensurate islands with two molecules per unit cell, possibly with different adsorption geometries. Second, at around 0.6 ML, the molecules arrange in disordered phases and form small chains with a length of only a few molecules. Finally, at 0.4 ML and below, most molecules adsorb isolated from each other in a disordered phase, whereby the molecular wings are well aligned with the high symmetry directions of the Cu(111) surface.[18] In the investigated temperature range (140–300 K), no phase transitions of the lateral structure were observed.

We performed NIXSW measurements in all coverage ranges in question. The results are displayed in Fig. 4: C1s and N1s photoelectron yield curves with corresponding reflectivity measurements. The Cu2p signal of the molecules cannot be distinguished from the bulk signal and therefore it was not measured.

The fitting results (coherent positions P^H and fractions F^H) are given in Fig. 4, and again plotted in a real-scale model in Fig. 5. In clear contrast to CuPc/Au(111), the van der Waals radii strongly overlap, indicating a rather strong chemisorptive interaction with the substrate. The bonding distances (in Å) are clearly smaller than what was observed for the Ag substrate,[32] and in the same range as the values for the carbon backbone of the PTCDA monolayer structure on Cu(111).[28] However, here we also observed an effect on the adsorption height caused by different coverages. For the highest coverage of 0.9 ML, D^H increases by 0.2–0.3 Å for both species and both temperatures, compared to the 0.4 and 0.6 ML structures; see Fig. 5. The coherent fractions also show a rather clear trend: For decreasing coverages, the values for F^H shift from smaller to higher values (0.3–0.6 for C1s; 0.5–0.7 for N1s). This might indicate that at low coverages the molecules obtain a smaller number of inequivalent adsorption sites, which are possibly also better defined and more stable than at higher coverages; see discussion below.

IV. DISCUSSION

Together with the results for the lateral geometric structure and the electronic valence structure (see Ref. 33), this work enables a comprehensive understanding of the interactions between the CuPc molecules and the Au, Ag, and Cu(111)-oriented surfaces. In this row, the adsorption on Au and Cu represents the most extreme cases of weak physisorption and rather strong chemisorption, respectively.

On Au(111), we found adsorption heights which are in good agreement with nonbonding contact distances from literature[37] (see Fig. 3). This indicates the dominant role of the van der Waals interaction, and that no significant intermixing of states, hybridization, or charge transfer occurs in this case. Our finding is also in agreement with ultraviolet photoemission (UPS) experiments, which showed no indications for a (partially) occupied state close to the Fermi edge that could be interpreted as a former lowest unoccupied molecular orbital (LUMO).[33] Furthermore, it is in agreement with the lateral structure formation which was found by electron diffraction experiments, as the molecules form only point-on-line coincident, or incommensurate structures. This indicates that the influence of the substrate on the structure formation is small or even negligible. The occurrence of point-on-line structures results from the minimization of the interface potential energy. For weakly interacting systems, it was demonstrated [for the example of TiOPc on Au(111)] that such point-on-line superstructures can be caused by a mere Lennard-Jones–type potential.[40]

These findings let us conclude that the bonding to the Au substrate is—in contrast to the adsorption on Ag(111) or Cu(111)—not site specific. It explains the observation of constant adsorption heights and very similar bonding strengths

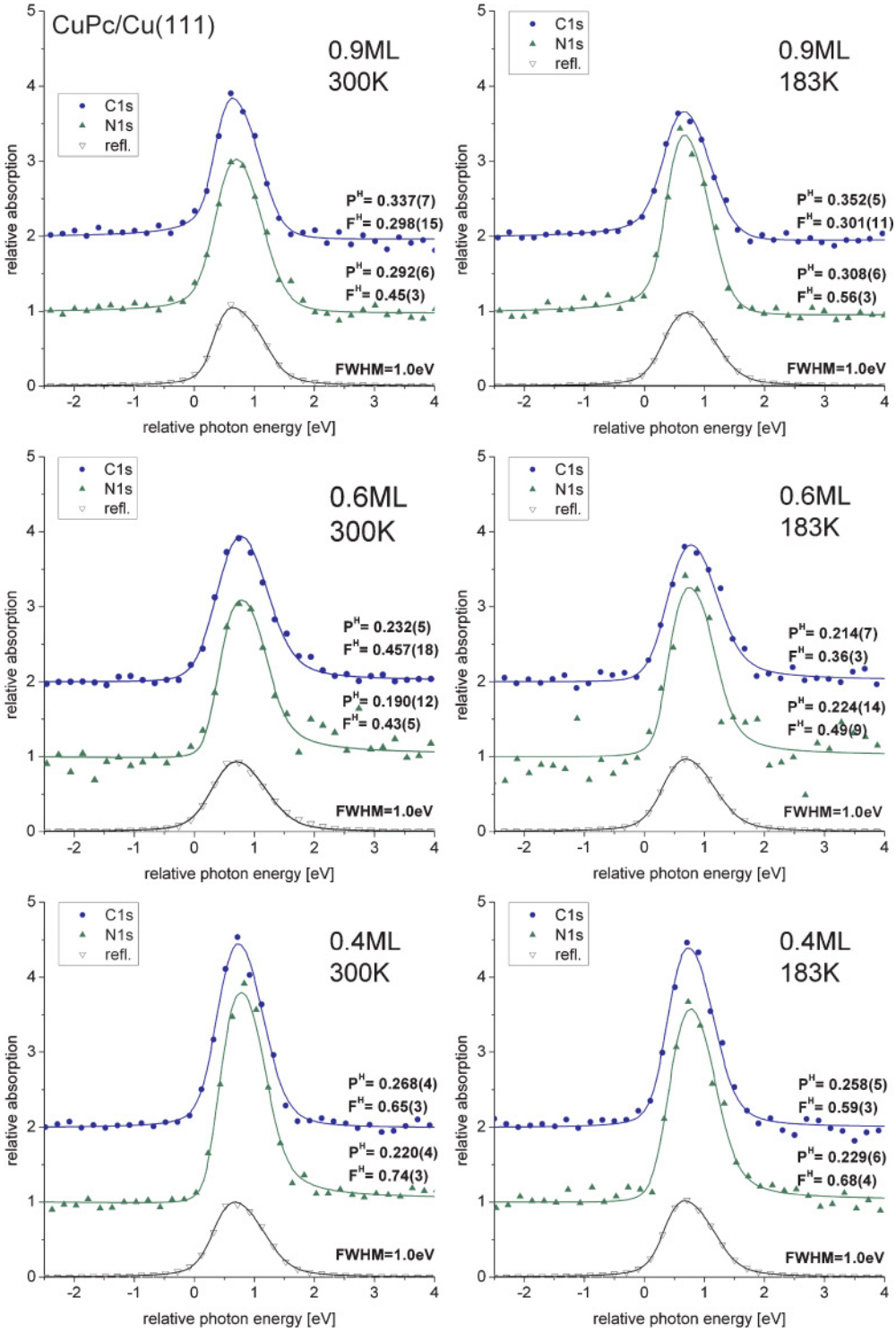

FIG. 4. (Color online) Photoelectron yield and reflectivity curves for CuPc/Cu(111) (summed individual scans). The errors given here stem from the χ^2 fitting from the GMinuit algorithm in Root. More realistic values are given in Fig. 5; see also the end of Sec. II and Ref. 32.

in all phases occurring for CuPc/Au(111) in the submonolayer range.[32]

On Cu(111), we observed adsorption heights that indicate a significant overlap of molecular and substrate electronic states, implicating intermixing of states, hybridization, and charge transfer. In fact, UPS spectra clearly show the occupation of a former LUMO state.[33] The structural models obtained from spot profile analysis LEED[33] and STM[18] indicate a strong tendency of the molecules to obtain only one (or very few) adsorption sites and form commensurate superstructures. This is strong evidence for a very local bonding mechanism involving hybridization, for which a spatial overlap of molecular and substrate electronic states is essential.

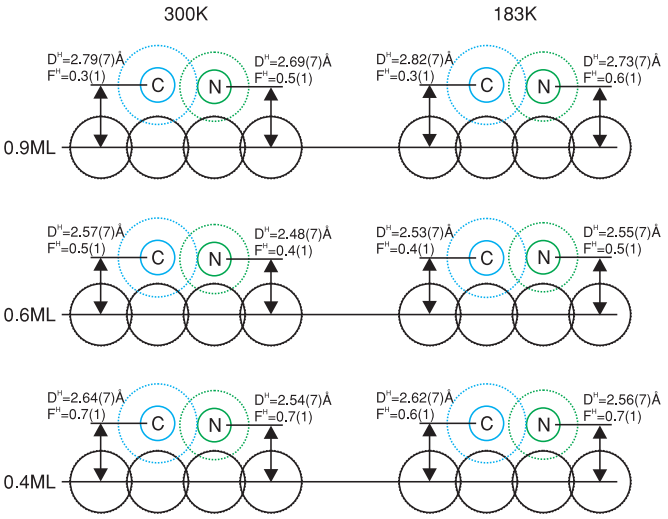

FIG. 5. (Color online) On-scale adsorption model for CuPc/Cu(111). The dotted and full circles denote van der Waals[37] and covalent bonding radii,[38] respectively.

We have also found a trend to larger adsorption heights for the CuPc molecules at high coverages; see above. This indicates that the bonding strength depends on the density of the molecules on the surface and on the lateral structure. An—on average—weaker bonding of the molecules in the commensurate phase at 0.9 ML, which has two molecules per unit cell,[33] can easily be explained by two different adsorption sites of the molecules as they have been found for this structure. The different sites are due to an electrostatically induced azimuthal misalignment of one molecule with the substrate high-symmetry axes.[33] This misaligned molecule has a larger adsorption height and causes the higher coherent position that we measured, since P^H is given by the superposition of both molecular adsorption geometries. Hence the large density of molecules, which causes the formation of the commensurate 0.9 ML phase, does not allow that all molecules obtain identical adsorption sites. Half of them are displaced and (as STM images show) also rotated, so that they cannot take their "ideal" adsorption geometry. This interpretation is underlined by the reduced coherent fraction of the 0.9 ML structure compared to the 0.4 and 0.6 ML structures.

Consequently, this structure consists of one more strongly bonded molecule, well aligned with the substrate high-symmetry directions, and a second one in the same unit cell which is misaligned and more weakly bonded. The lateral structure and intermolecular interaction is responsible for a weakening of the bonding of the latter molecules. Such an influence of the adsorption site on the bonding strength has also been found for PTCDA/Ag(111) in scanning tunneling spectroscopy measurements. In the spectra, different features occur close to the Fermi level for isolated molecules, for the two inequivalent molecules in the unit cell of the herringbone phase, and for molecules in the low-temperature phase.[9,41]

Compared to the two cases discussed so far—CuPc on Au(111) and Cu(111)—the adsorption on Ag(111) represents an "intermediate" case, at least on the first view. Similar to the situation on Cu(111), we also found charge transfer between molecule and substrate (indicated by a half-filled

TABLE II. Comparison of adsorption heights of CuPc submonolayers on Au, Cu, and Ag(111) at LT, in units of the sum of van der Waals radii of the corresponding species. van der Waals radii are taken from Ref. 37: $r_{Au} = 1.66$ Å, $r_{Ag} = 1.72$ Å, $r_{Cu} = 1.4$ Å, $r_C = 1.77$ Å, and $r_N = 1.55$ Å.

Substrate	Cov (ML)	D_{C1s} (%)	D_{N1s} (%)	D_{Cu2p} (%)
Au(111)	1.00	96(2)	102(2)	108(2)
	0.70	98(2)	101(2)	106(2)
Ag(111)	1.00	88(1)	94(2)	97(2)
(Ref. 32)	0.85	86(1)	92(2)	94(2)
	0.50	86(1)	90(2)	93(2)
Cu(111)	0.90	89(2)	93(2)	
	0.60	80(2)	86(2)	
	0.40	83(2)	87(2)	

former LUMO), which involves intermixing of states and hybridization.[32] The phase diagram looks very similar to CuPc/Cu(111), with one very important difference: Within the point-on-line regime (coverage > 0.9 ML), a full series of structures occurs which shows a continuously shrinking unit cell with increasing coverage. This effect was interpreted as intermolecular repulsion caused by donation and back-donation of electronic charge between molecules and substrate.[19,32] Regarding adsorption heights, earlier NIXSW measurements revealed absolute values in the range of 3.0 Å for all coverages between 0.5 and 1.0 ML, with a clear trend to higher values (i.e., weaker bonding) for higher coverages, similar to what is reported here for CuPc/Cu(111).

Comparing the naked absolute adsorption heights measured for CuPc/Au(111) (≈3.3 Å), Ag(111) (≈3.0 Å), and Cu(111) (≈2.7 Å), one might conclude that the interaction strength clearly increases for the row of substrates Au-Ag-Cu. However, for a fair comparison, bonding distances have to be normalized to the size of the atoms involved in the bonding. While Ag and Au atoms are of comparable size, Cu atoms are significantly smaller, which relativizes the apparently stronger bonding on this substrate. In Table II, we list the adsorption heights of all species C, N, and Cu above the substrates Au(111), Ag(111), and Cu(111) in units normalized to the sum of the van der Waals radii of the corresponding atoms. We have selected the LT phases only for this comparison, since in most cases no significant temperature dependency was found. The table clearly shows different bonding distances for Au(111) on the one side (99.3% as averaged from all C-Au and N-Au distances) and Ag(111) and Cu(111) on the other side (89.3% for Ag and 86.3% for Cu), which illustrates the difference between physisorption for CuPc/Au(111) and chemisorption for CuPc/Ag(111) and Cu(111). However, it also shows that the difference in the interaction strength between CuPc/Cu(111) and CuPc/Ag(111) is not as large as one might believe from the naked Å values. For the 1.0 ML phases, the values are even almost identical.

However, it is fact that spectroscopic data indicate a significantly stronger charge transfer for CuPc on Cu(111) compared to Ag(111), even for the monolayer regime, and that the structures which are formed in the high-coverage regime at > 0.9 ML [basically only one commensurate structure on Cu(111), but a continuous series of p.o.l. structures on

Ag(111)] clearly suggest a more site-specific adsorption geometry on Cu.[33] This alleged contradiction might be explained by the number of substrate atoms interacting with one molecule. Since the surface area per molecule in the monolayer structure is nearly identical on Ag(111) (192 Å) and Cu(111) (193 Å), the number of substrate atoms lying below one molecule differs due to the smaller lattice of Cu. One molecule corresponds to ≈ 34 Cu atoms, but only ≈ 26.5 Ag atoms. This enables a more effective interaction of molecular and substrate electronic states for the adsorption on Cu(111); however, for a more detailed discussion, reliable quantum chemical calculations were necessary which are difficult, not only because the structures are incommensurate.

Finally, we want to mention that the coverage-induced change of the adsorption height, i.e., the trend to weaker molecule-substrate bonding at higher coverage, is clearly stronger for the system CuPc/Cu(111) than for CuPc/Ag(111). On Ag(111), the adsorption height changes by about 2%–4% when isolated molecules are compared with those in the p.o.l. structures. On Cu(111), the corresponding change is roughly doubled (5%–8%), while on the Au(111) surface no such effect was found. This observation allows one to conclude that the effect of coverage-induced weakening of the bonding is strengthened for a more strongly interacting system. This underlines the impact of the local, site-specific bonding on the structure formation of large π-conjugated molecules on weakly interacting noble metal surfaces, and vice versa, i.e., the influence of the lateral structure formation on the interaction across metal-organic interfaces.

V. SUMMARY

We investigated the influence of the (lateral) geometric structure of a (sub)monolayer film of CuPc on the (vertical) adsorption height of the molecules on Au(111), Ag(111), and Cu(111) surfaces. On the reconstructed Au(111) surface, isolated molecules occur in a disordered phase at low coverage and an ordered p.o.l. structure at higher coverage. In all cases, the molecules show almost identical adsorption heights close to the sum of the van der Waals radii of the atomic species involved. This indicates a pure physisorptive and not site-specific adsorbate-substrate interaction. In contrast, CuPc on Cu(111) shows a rather strong chemisorptive bonding with the molecules either isolated or aligned in small chains for the low submonolayer coverage regime. At higher coverage a commensurate long-range-ordered superstructure occurs, which shows a significantly weaker interaction to the substrate, probably caused by two inequivalent adsorption sites per unit cell. The results were compared in detail with similar results for CuPc/Ag(111),[32] which is an intermediate case in terms of substrate bonding. An increase of interaction strength was found for the row CuPc/Au(111)-Ag(111)-Cu(111), whereby the difference for the adsorption on Ag and Cu must be seen in the perspective of the different size of Ag and Cu atoms. Furthermore, the weakening of the bonding with increasing coverage was investigated and compared for the three systems. Obviously, this effect scales with the overall interaction strength, i.e., it is strongest for strongly interacting systems like CuPc/Cu(111).

ACKNOWLEDGMENTS

We would like to thank the ESRF and their staff members Yanyu Mi, Blanka Detlefs, and Jörg Zegenhagen for enabling the NIXSW experiments and their permanent support during the beamtime. We also acknowledge Patrick Bayersdorfer and Giuseppe Mercurio for their help, as well as Marc Häming, Johannes Ziroff, and Christoph Stadler for stimulating discussions. This work was supported by the Deutsche Forschungsgemeinschaft (KU 1531/2-1).

[1] Y. R. Sun, N. C. Giebink, H. Kanno, B. W. Ma, M. E. Thompson, and S. R. Forrest, Nature (London) **440**, 908 (2006).
[2] M. Eremtchenko, J. A. Schäfer, and F. S. Tautz, Nature (London) **425**, 602 (2003).
[3] F. Schreiber, Prog. Surf. Sci. **65**, 151 (2000).
[4] F. S. Tautz, Prog. Surf. Sci. **82**, 479 (2007).
[5] A. Abbasi and R. Scholz, J. Phys. Chem. C **113**, 19897 (2009).
[6] S. Duhm, A. Gerlach, I. Salzmann, B. Broeker, R. L. Johnson, F. Schreiber, and N. Koch, Org. Electron. **9**, 111 (2008).
[7] A. Hauschild, K. Karki, B. C. C. Cowie, M. Rohlfing, F. S. Tautz, and M. Sokolowski, Phys. Rev. Lett. **94**, 036106 (2005).
[8] A. Hauschild, R. Temirov, S. Soubatch, O. Bauer, A. Schöll, B. C. C. Cowie, T.-L. Lee, F. S. Tautz, and M. Sokolowski, Phys. Rev. B **81**, 125432 (2010).
[9] L. Kilian, A. Hauschild, R. Temirov, S. Soubatch, A. Schoell, A. Bendounan, F. Reinert, T. L. Lee, F. S. Tautz, M. Sokolowski, and E. Umbach, Phys. Rev. Lett. **100**, 136103 (2008).
[10] M. Rohlfing, R. Temirov, and F. S. Tautz, Phys. Rev. B **76**, 115421 (2007).
[11] C. Stadler, S. Hansen, A. Schöll, T.-L. Lee, J. Zegenhagen, C. Kumpf, and E. Umbach, New J. Phys. **9**, (2007).
[12] J. Stanzel, W. Weigand, L. Kilian, H. L. Meyerheim, C. Kumpf, and E. Umbach, Surf. Sci. **571**, L311 (2004).
[13] J. Ziroff, F. Forster, A. Schöll, P. Puschnig, and F. Reinert, Phys. Rev. Lett. **104**, 233004 (2010).
[14] Y. Zou, L. Kilian, A. Schöll, T. Schmidt, R. Fink, and E. Umbach, Surf. Sci. **600**, 1240 (2006).
[15] A. Gerlach, F. Schreiber, S. Sellner, H. Dosch, I. A. Vartanyants, B. C. C. Cowie, T. L. Lee, and J. Zegenhagen, Phys. Rev. B **71**, 205425 (2005).
[16] M. Häming, C. Scheuermann, A. Schöll, F. Reinert, and E. Umbach, J. Electron Spectrosc. Relat. Phenom. **174**, 59 (2009).
[17] K. W. Hipps, X. Lu, X. D. Wang, and U. Mazur, J. Phys. Chem. **100**, 11207 (1996).
[18] H. Karacuban, M. Lange, J. Schaffert, O. Weingart, Th. Wagner, and R. Moeller, Surf. Sci. **603**, L39 (2009).
[19] C. Stadler, S. Hansen, I. Kröger, C. Kumpf, and E. Umbach, Nature Phys. **5**, 153 (2009).

[20] Y. Wang, J. Kröger, R. Berndt, and W. Hofer, Ang. Chem. - Int. Ed. **48**, 1261 (2009).
[21] Y. Bai, I. Kröger, F. Bebensee, T.-L. Lee, J. Zegenhagen, H. P. Steinrück, C. Kumpf, and M. Gottfried (to be published).
[22] M. Häming, M. Greif, C. Sauer, A. Schöll, and F. Reinert, Phys. Rev. B **82**, 235432 (2010).
[23] B. W. Batterman, Rev. Mod. Phys. **36**, 681 (1964).
[24] J. J. Lee, C. J. Fisher, D. P. Woodruff, M. G. Roper, R. G. Jones, and B. C. C. Cowie, Surf. Sci. **494**, 166 (2001).
[25] D. P. Woodruff, Prog. Surf. Sci. **57**, 1 (1998).
[26] I. A. Vartanyants and J. Zegenhagen, Solid State Commun. **113**, 299 (1999).
[27] J. Zegenhagen, Surf. Sci. Rep. **18**, 199 (1993).
[28] A. Gerlach, S. Sellner, F. Schreiber, N. Koch, and J. Zegenhagen, Phys. Rev. B **75**, 045401 (2007).
[29] S. K. M. Henze, O. Bauer, T. L. Lee, M. Sokolowski, and F. S. Tautz, Surf. Sci. **601**, 1566 (2007).
[30] L. Romaner, D. Nabok, P. Puschnig, E. Zojer, and C. Ambrosch-Draxl, New J. Phys. **11**, 053010 (2009).
[31] C. Stadler, S. Hansen, F. Pollinger, C. Kumpf, E. Umbach, T. L. Lee, and J. Zegenhagen, Phys. Rev. B **74**, 035404 (2006).
[32] I. Kröger, B. Stadtmüller, C. Stadler, J. Ziroff, M. Kochler, A. Stahl, F. Pollinger, T. L. Lee, J. Zegenhagen, F. Reinert, and C. Kumpf, New J. Phys. **12**, 083038 (2010).
[33] B. Stadtmüller, I. Kröger, F. Reinert, and C. Kumpf, Phys. Rev. B **83**, 085416 (2011).
[34] J. Zegenhagen, B. Detlefs, T.-L. Lee, S. Thiess, H. Isern, L. Petit, L. Andre, J. Roy, Y. Mi, and I. Joumard, J. Electron Spectrosc. Relat. Phenom. **178**, 258 (2010).
[35] C. T. Chantler, J. Phys. Chem. Ref. Data **24**, 71 (1995).
[36] *International Tables for X-Ray Crystallography*, Vol. IV, edited by J. A. Ibers and W. C. Hamilton. (Kynoch Press, Birmingham, 1974).
[37] A. Bondi, J. Phys. Chem. **68**, 441 (1964).
[38] [www.webelements.com].
[39] A. R. Sandy, S. G. J. Mochrie, D. M. Zehner, K. G. Huang, and D. Gibbs, Phys. Rev. B **43**, 4667 (1991).
[40] S. C. B. Mannsfeld and T. Fritz, Phys. Rev. B **71**, 235405 (2005).
[41] A. Kraft, R. Temirov, S. K. M. Henze, S. Soubatch, M. Rohlfing, and F. S. Tautz, Phys. Rev. B **74**, 041402 (2006).